Actin-dependent localization of an RNA encoding a cell-fate determinant in yeast

Peter A. Takizawa*†, Anita Sil‡, Jason R. Swedlow†, Ira Herskowitz‡ & Ronald D. Vale*†‡

** Howard Hughes Medical Institute, and Departments of † Cellular and Molecular Pharmacology and ‡ Biochemistry and Biophysics, University of California, San Francisco, California 94143-0450, USA*

The cytoplasmic localization of messenger RNA creates an asymmetric distribution of proteins that specify cell fate during development in multicellular eukaryotes[1,2]. The protein Ash1 is a cell-fate determinant in budding yeast which localizes preferentially to the presumptive daughter nucleus, where it inhibits mating-type switching[3,4]. Here we show that Ash1 mRNA is localized to the distal tip of daughter buds in post-anaphase cells. Three-dimensional imaging reveals that Ash1 mRNA is assembled into particles that associate with the cell cortex. To achieve this localization, Ash1 mRNA must have its 3′ untranslated region and the actin cytoskeleton must be intact. Ash1 mRNA is not localized correctly in the absence of a myosin (Myo4) and is mislocalized to the mother-bud neck in the absence of a regulator of the actin cytoskeleton known as Bni1. We propose that Ash1 mRNA particles are transported into the daughter bud along actin filaments and are anchored at the distal tip. Thus, as in higher eukaryotes, *Saccharomyces cerevisiae* employs RNA localization to generate an asymmetric distribution of proteins and hence to determine cell fate.

Transcription of the *ASH1* gene and translation of its RNA occur in large-budded cells that have undergone nuclear division but not cytokinesis[3,4]. In these post-anaphase cells, Ash1 protein localizes preferentially to the nucleus in the bud (incipient daughter cell). In principle, asymmetric localization of Ash1 protein could result from restriction of *ASH1* transcription to the incipient daughter nucleus, accumulation of Ash1 mRNA in the incipient daughter cell, or accumulation of Ash1 protein in the incipient daughter as a result of a localization determinant on the protein itself.

To determine whether Ash1 mRNA accumulates in the incipient daughter cell, we looked at the subcellular location of Ash1 mRNA by *in situ* analysis. Standard FISH (fluorescent *in situ* hybridization) techniques were inadequate to detect endogenous Ash1 mRNA. However, by combining a hybridization step employing digoxigenin-labelled antisense RNA probes with an antibody sandwiching procedure, the fluorescent signal was increased sufficiently so that endogenous Ash1 mRNA (Fig. 1), as well as several other RNAs tested (data not shown), could be easily imaged by fluorescence microscopy. Cells deleted for the *ASH1* gene showed only background straining, indicating that the signal was specific (Fig. 1). In an asynchronous population, only the large-budded cells with two distinct DAPI-stained nuclei (indicative of post-anaphase cells) displayed Ash1 mRNA staining (Fig. 1). Synchronization of cells by release from α-factor arrest revealed that the Ash1 mRNA signal peaked in post-anaphase cells and then rapidly declined (data not shown). The presence of Ash1 mRNA in only these cells is consistent with previous results from northern blotting analysis indicating that Ash1 mRNA accumulates in late anaphase and disappears soon afterwards[3]. Most significantly, the enhanced FISH staining pattern revealed that Ash1 mRNA was concentrated at the distal tip of large buds (Fig. 1). The fidelity of this localization was high: 91% of cells had tightly localized Ash1 mRNA at the distal tip, with virtually no signal in the mother cell; 7% had delocalized mRNA confined to the bud; and only 3% showed significant staining in the mother cell ($n = 100$).

We also examined cells that overexpress *ASH1* and detected not only staining at the distal tip but also significant amounts of unlocalized Ash1 mRNA in both the mother cell and bud (data not shown). This is consistent with the finding that Ash1 protein is

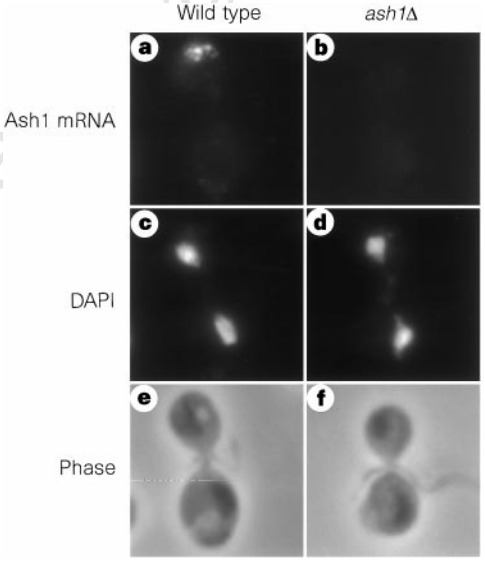

Figure 1 Ash1 mRNA is localized to the distal tip of the presumptive daughter cell. Isogenic wild-type cells (YAS140) (**a**, **c**, **e**) and *ash1*Δ cells (YAS145) (**b**, **d**, **f**) were grown to early log phase, fixed and probed for Ash1 RNA by FISH (**a**, **b**). DNA staining by DAPI (4,6-diamino-2-phenylindole) fluorescence (**c**, **d**) and phase-contrast images (**e**, **f**) indicate that Ash1 mRNA is stained during post-anaphase.

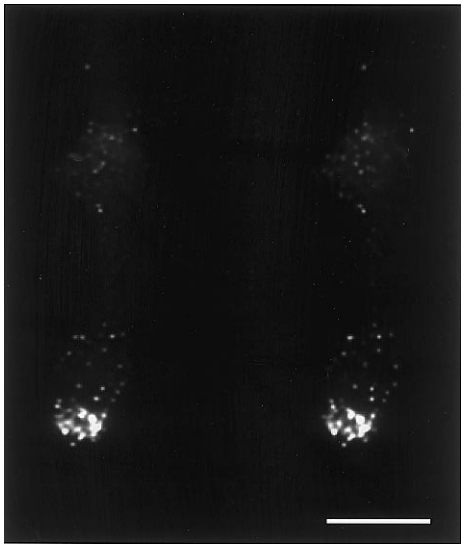

Figure 2 Three-dimensional reconstruction of Ash1 mRNA-containing particles. The image is presented as a stereo pair. To study a uniform population of cells, post-anaphase cells were accumulated by arresting cells with α-factor and then incubated for 60 min in pheromone-free medium. Cells were fixed and processed by FISH to detect Ash1 mRNA. Wide-field optical sectioning and constrained, iterative deconvolution were performed to generate a three-dimensional reconstruction. The background is increased to allow visualization of the mother cell. Scale bar, 5 μm.

found in both mother and daughter nuclei of cells overexpressing Ash1 (ref. 4). Because overexpression of *ASH1* caused abnormal localization, we visualized Ash1 mRNA from the chromosomal *ASH1* gene in all of the experiments described below.

To study the intracellular distribution of Ash1 mRNA at higher resolution, we imaged FISH staining patterns by wide-field optical sectioning microscopy and three-dimensional image restoration[5,6]. This imaging technique revealed that Ash1 mRNA was organized into diffraction-limited (<200 nm) particles (Fig. 2), as found for other localized mRNAs[7–9]; moreover, the particles were clearly localized near the cortex. Even the minority of particles that were not at the distal tip were also located adjacent to the cell membrane (Fig. 2).

To investigate how Ash1 mRNA is transported to and then maintained at the bud tip, we studied Ash1 mRNA localization in mutant strains deleted for the genes *SHE1–SHE5*, which are required for proper localization of Ash1 protein[3,10]. Three of these genes encode proteins that interact with or influence the actin cytoskeleton: *SHE1* encodes a putative actin-based myosin motor, Myo4 protein[10]; *SHE5* encodes Bni1 protein, which is involved in promoting actin-filament formation and polarization[10]; and *SHE4* encodes an uncharacterized protein necessary for proper polarization of the actin cytoskeleton[11]. In strains deleted for *MYO4/SHE1*, *SHE2*, *SHE3* or *SHE4*, the Ash1 mRNA particles were distributed throughout the mother and daughter compartments of large-budded cells (Fig. 3, and data not shown). In contrast, in *bni1Δ/she5Δ* cells, Ash1 RNA accumulated in the mother-bud neck region of post-anaphase cells (Fig. 3). In a strain lacking both *MYO4/SHE1* and *BNI1/SHE5*, Ash1 mRNA was mislocalized in a way indistinguishable from that observed in the *myo4Δ/she1Δ* strain (data not shown). Thus, four of the *she* mutant strains were incapable of localizing Ash1 mRNA, whereas in the *bni1Δ/she5Δ* strain, Ash1 mRNA was localized to the neck instead of to the distal tip.

Analysis of the *she* mutants suggested that the actin cytoskeleton might play a role in localizing Ash1 mRNA. To test the requirement for actin filaments in Ash1 mRNA localization, wild-type cells were treated with the actin-depolymerizing agent latrunculin A[12]. After a 5-min incubation with 200 μM latrunculin A, the actin cytoskeleton was completely disrupted and Ash1 mRNA was randomly distributed throughout the presumptive mother and daughter compartments (Fig. 4). Latrunculin A also affected the asymmetric accumulation of Ash1 protein; after a 5-min incubation, 70% of larger-budded, post-anaphase cells had equivalent Ash1 protein staining in both mother and daughter nuclei (symmetric staining), 21% had more Ash1 protein in the daughter nucleus than in the mother (partially symmetric), and only 9% showed Ash1 protein exclusively in the daughter nucleus (asymmetric staining) ($n = 100$). Control cells, in contrast, showed 10% symmetric staining, 19% partially symmetric staining and 71% asymmetric staining ($n = 100$). In cells treated with the microtubule-depolymerizing agent nocodazole (50 μM), microtubules were absent but Ash1 mRNA was still localized to the distal tip of daughter cells (data not shown). Thus, perturbation of the actin cytoskeleton, but not microtubules, disrupts Ash1 mRNA localization and Ash1 protein asymmetry.

In higher eukaryotes, mRNA localization is specified by sequence elements in the 3′ untranslated region (UTR)[1,2]. To see whether the *ASH1* 3′UTR is required for Ash1 mRNA localization, we integrated an allele of *ASH1* lacking its 3′UTR at the *ASH1* locus. Ash1 mRNA expressed from the 3′UTRΔ allele failed to localize to the distal tip; instead it was distributed as particles throughout the mother and daughter (Fig. 3). Furthermore, in 3′UTRΔ cells, the normal

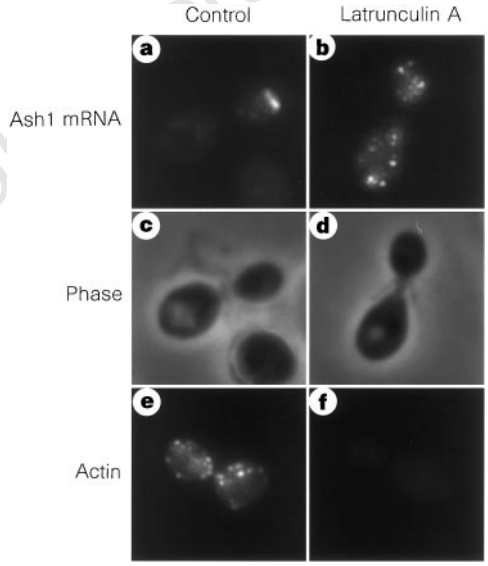

Figure 4 The actin cytoskeleton is required for Ash1 mRNA localization. Cells (YAS140) were grown to early log phase and treated with 200 μM latrunculin A/2% DMSO (**b**, **d**, **e**), or an equivalent amount of DMSO (**a**, **c**, **f**), for 5 min, fixed and probed for Ash1 mRNA by FISH (**a**, **b**). An aliquot of each sample was removed after fixation and stained with rhodamine phalloidin[16] to demonstrate that actin filaments are completely depolymerized by this treatment (**e**, **f**).

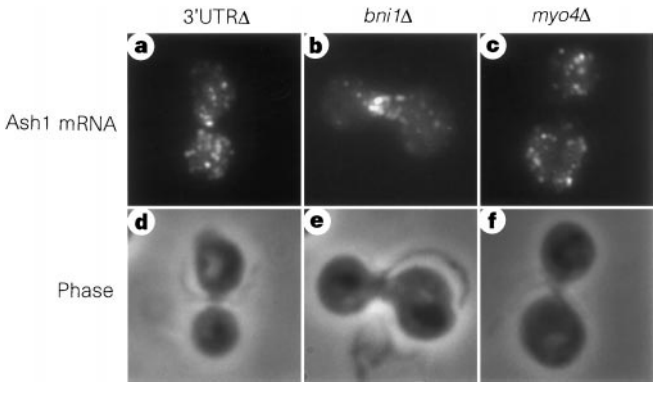

Figure 3 Ash1 mRNA localization requires its 3′UTR and the cytoskeletal proteins, Bni1 and Myo4. 3′UTRΔ (YAS222) (**a**, **d**), *she5Δ/bni1Δ* (YAS219-1A) (**b**, **e**), and *she1Δ/myo4Δ* (YAS217-1A) (**c**, **f**) were grown to early log phase, fixed and probed for Ash1 mRNA by FISH (**a**, **b**, **c**). The corresponding phase-contrast images are shown (**d**, **e**, **f**).

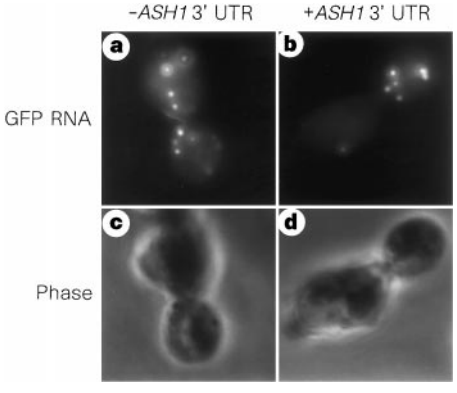

Figure 5 The *ASH1* 3′UTR is sufficient for asymmetric RNA localization to the bud. *ash1Δ* cells (YAS145) carrying either *pPHO4-GFP* (EB0359) (**a**, **c**) or *pPHO4-GFP* fused to the *ASH1* 3′UTR (pPT100) (**b**, **d**) were synchronized (see Methods) and subjected to FISH analysis (**a**, **b**). The corresponding phase images are shown (**c**, **d**).

asymmetry of Ash1 protein was markedly disrupted: 80% of large-budded, post-anaphase cells showed symmetric staining, 5% showed partially symmetric staining, and only 15% showed asymmetric staining ($n = 200$). Wild-type cells, in contrast, gave only 4% symmetric cells, 19% partially symmetric cells and 77% exclusively asymmetric cells ($n = 200$). Thus, the 3′UTR is required for proper localization of Ash1 mRNA and protein.

We next investigated whether the *ASH1* 3′UTR was sufficient to localize a heterologous RNA to daughter cells. Cells were transformed with a plasmid encoding either green fluorescent protein (GFP) or GFP fused to a 564-nucleotide fragment containing the *ASH1* 3′UTR. The GFP mRNA was detected by FISH in a synchronized population of large-budded cells. We found that 65% of the cells containing the GFP–*ASH1* 3′UTR fusion showed asymmetric localization of GFP mRNA to the daughter cell ($n = 100$) (Fig. 5). In contrast, GFP mRNA without the *ASH1* 3′UTR was asymmetrically localized in only 6% of cells ($n = 100$) (Fig. 5). Shorter regions of the *ASH1* 3′UTR fused to GFP (the 5′ and 3′ 282-nucleotide halves of the 3′UTR fragment described above) likewise failed to localize asymmetrically (not shown). Although the *ASH1* 3′UTR was sufficient to confer asymmetric localization of GFP mRNA to the bud, the GFP mRNA failed to concentrate at the distal tip as seen for Ash1 mRNA. Thus, it appears that the *ASH1* 3′UTR can specify transport to daughter cells, but other sequences in Ash1 mRNA may be required to anchor it at the distal tip.

We have shown that Ash1 mRNA is localized to the distal tip of the incipient daughter cell. Under conditions in which Ash1 mRNA localization is disrupted (as a result of overexpression of *ASH1*, deletion of the 3′UTR or treatment with latrunculin A, or in *she* mutant strains), Ash1 protein accumulates symmetrically in both mother and daughter nuclei. We therefore propose that asymmetric localization of the cell-fate determinant Ash1 results from localization of its mRNA. Rapid localization of Ash1 mRNA to the distal pole of the predivisional cell might be sufficient to restrict most Ash1 to the daughter-cell nucleus; once the mRNA is translated, most of the resultant protein will translocate into the most proximal nucleus.

Our results suggest that Ash1 mRNA localization occurs as a result of transport of RNA-containing particles along actin filaments to the distal tip of the bud. We propose that movement of RNA to the distal pole may be very rapid, because synchronized cells do not show a well defined intermediate population of cells with RNA particles in transit to the bud. Once at the distal pole, the RNA might be tethered to the cortex by interactions with an anchor protein. In *bni1Δ* cells, the anchor protein may be trapped at the mother-bud neck, thereby sequestering Ash1 mRNA at an inappropriate site. None of the She proteins is localized exclusively to the distal tip at the time Ash1 mRNA accumulates[10], suggesting that the anchor protein is yet to be identified.

The mechanism of mRNA localization in *S. cerevisiae* appears to be similar to that in higher eukaryotes, in which microtubules and actin filaments have been implicated in the transport and anchoring of RNA[9,13–15]. The ease of genetic and biochemical manipulation of *S. cerevisiae* makes it a propitious system for determining the details of how mRNA is localized. Moreover, our results suggest that other yeast proteins involved in cell-fate determination or bud formation may be asymmetrically distributed by transport and localization of their mRNAs.

Note added in proof: Another report of Ash1 mRNA localization appeared while this Letter was under review[17]. □

Methods

Yeast strains. All strains were derived from YAS140 which is W303a (K699: ***a*** *ura3-1 his3-11,15 trp1-1 leu2-3,112 ade2-1 can1-100*). YAS145: ***a*** *ash1ΔLEU2*. YAS217-1A: ***a*** *she1ΔURA3*. YAS218-1D: **a** *she3ΔURA3*. YAS219-1A: **a** *she5ΔURA3*. YAS220-1B: **a** *she2ΔURA3*. YAS221-3A: ***a*** *she4ΔURS3*. YAS222: **a** *ash1ΔLEU2::ASH1-3′UTRΔ-URA3*. (YAS222 contains an allele of *ASH1* that lacks its 3′UTR; this allele has been integrated at the *ASH1* locus in place of the wild-type gene.) The following strains were a kind gift from R. P. Jansen and K. Nasmyth: YAS171 (K5102: ***a***/α *SHE5/she5::URA3*); *YAS172* (*K5104:* ***a***/α *SHE1/she1::URA3*); YAS173 (K5213; ***a***/α *SHE3/she3::URA3*); *YAS174 (K5477:* α *she2::URA3*); YAS175 (K5560: α *she4::URA3*).

Sample preparation and enhanced FISH. Cultures were grown to OD_{600}∼0.5 and fixed in 4% formaldehyde for 1 h. Cells were washed and spheroplasted in 100 mM potassium phosphate buffer, pH 7.0, 1.2 M sorbitol containing 30 mM β-mercaptoethanol and 40 μg ml^{-1} zymolyase 100T (ICN Biomedicals) for 15 min at 37 °C. Cells were washed and spread on polylysine-coated, multiwell test slides. Cells were incubated for 1 h in hybridization mix (50% formamide, 5 × SSC, 1 mg ml^{-1} yeast tRNA, 100 μg ml^{-1} heparin, 1 × Denhardt's, 0.1% Tween-20, 0.1% CHAPS, and 5 mM EDTA), then incubated overnight at 37 °C in hybridization mix containing 5 μg ml^{-1} Ash1 probe. Ash1 probe was prepared by generating digoxigenin-labelled, antisense Ash1 RNA with Megascript Kit (Ambion) according to the manufacturer's protocol. The resultant digoxigenin-labelled RNA was subjected to alkaline hydrolysis to generate ∼0.25-kb fragments. After hybridization, cells were washed in 0.2 × SSC and blocked in PBS, 0.1% Triton X-100, 10% horse serum. Cells were incubated with mouse anti-digoxigenin antibody (Boehringer-Mannheim) diluted to 0.4 μg ml^{-1} in blocking buffer for 2 h. After washing in PBS, cells were incubated with rabbit anti-mouse IgG diluted to 1 μg ml^{-1} in blocking buffer for 1 h. After washing, cells were incubated with rhodamine-conjugated goat anti-rabbit IgG (ICN Pharmaceuticals). Cells were washed and mounted in 0.01 M Tris-Cl, pH 8.4, 90% glycerol, 1 mg ml^{-1} *p*-phenylenediamine, and 0.1 μg ml^{-1} DAPI (Sigma). We also used a second detection method that results in a considerably stronger signal: after overnight hybridization and washing, cells were incubated with anti-digoxigenin coupled to alkaline phosphatase (Boehringer-Mannheim). A fluorescent precipitate was generated using an HNPP fluorescent detection kit (Boehringer-Mannheim).

Synchronized cells were generated by growing cells to $OD_{600} = 0.3$. α-Factor was added to 20 μg ml^{-1} and cultures were incubated for 3 h at 30 °C. Cells were washed twice in YPD and incubated for 60 min at 30 °C. Cells were fixed and processed as described.

Microscopy. Samples were viewed under a Nikon EFD-3 microscope using a 100×/NA 1.4 lens. Images were captured with a cooled charge-coupled device, and digital images were displayed using Adobe Photoshop. Wide-field optical sectioning and image deconvolution were performed by collecting optical sections with a Nikon 100×/NA 1.4 lens at 0.2-μm intervals on a wide-field microscopy workstation equipped with a Peltier-cooled charge-coupled device (Kodak) mounted in a scientific imaging camera (Photometrics)[5]. Images were restored by constrained, iterative deconvolution[6]. This method uses an empirical measurement of the image blurring caused by the microscope objective lens to restore out-of-focus photons to their correct position. Stereo pairs were calculated by summing pixel values along projection rays[5].

Received 23 June; accepted 7 August 1997.

1. St Johnston, D. The intracellular localization of messenger RNAs. *Cell* **81,** 161–170 (1995).
2. Willhelm, J. E. & Vale, R. D. RNA on the move: the mRNA localization pathway. *J. Cell Biol.* **123,** 269–274 (1993).
3. Bobola, N., Jansen, R.-P., Shin, T. H. & Nasmyth, K. Asymmetric accumualtionof Ash1p in postanaphase nuclei depends on a myosin and restricts yeast mating-type switching to mother cells. *Cell* **84,** 699–709 (1996).
4. Sil, A. & Herskowitz, I. Identification of an asymmetrically localized determinant, Ash1p, required for lineage-specific transcription of the yeast *HO* gene. *Cell* **84,** 711–722 (1996).
5. Swedlow, J. R., Sedat, J. W. & Agard, D. A. in *Deconvolution of Images and Spectra* 2nd edn 284–309 (Academic Press, New York, 1997).
6. Agard, D. A., Hiraoka, Y., Shaw, P. & Sedat, J. W. *Meth. Cell Biol.* **30,** 353–366 (1989).
7. Ainger, K. *et al.* Transport and localization of exogenous myelin basic protein mRNA microinjected into oligodendrocytes. *J. Cell Biol.* **123,** 431–441 (1993).
8. Taneja, K. L., Lifshitz, L. M., Fay, F. S. & Singer, R. H. Poly(A) RNA codistribution with microfilaments: evaluation by *in situ* hybridization and quantitative digital imaging microscopy. *J. Cell Biol.* **119,** 1245–1260 (1992).
9. Ferrandon, D., Elphick, L., Nusslein-Volhard, C. & St Johnston, D. Staufen protein associates with the 3′UTR of bicoid mRNA to form particles that move in a microtubule-dependent manner. *Cell* **79,** 1221–1232 (1994).
10. Jansen, R.-P., Dowzer, C. ,Michaelis, C., Galova, M. & Nasmyth, K. Mother cell-specific *HO* expression in budding yeast depends on the unconventional myosin Myo4p and other cytoplasmic proteins. *Cell* **84,** 687–697 (1996).
11. Wendland, B., McCaffery, J. M., Xiao, Q. & Emr, S. D. A novel fluorescence-activated cell sorter-based screen for yeast endocytosis mutants identifies a yeast homologue of mammalian eps15. *J. Cell Biol.* **135,** 1485–1500 (1996).
12. Ayscough, K. R. *et al.* High rates of actin filament turnover in budding yeast and roles for actin in establishment and maintenance of cell polarity revealed using the actin inhibitor latrunculin-A. *J. Cell Biol.* **137,** 399–416 (1997).

13. Yisraeli, J. K., Sokol, S. & Melton, D. A. A two-step model for the localization of maternal mRNA in *Xenopus* oocytes: involvement of microtubules and microfilaments in the translocation and anchoring of Vg1 mRNA. *Development* **108,** 289–298 (1990).
14. Sundell, C. L. & Singer, R. H. Requirement of microfilaments in sorting of actin messenger RNA. *Science* **253,** 1275–1277 (1991).
15. Pokrywka, N. J. & Stephenson, E. C. Microtubules are a general component of mRNA localization systems in *Drosophila* oocytes. *Dev. Biol.* **167,** 363–370 (1995).
16. Adams, A. E. M. & Pringle, J. R. in *Guide to Yeast Genetic and Molecular Biology* 729–731 (Academic Press, New York, 1991).
17. Long, R. M. *et al.* Mating type switching in yeast controlled by asymmetric localization of *ASH1* mRNA. *Science* **277,** 383–387 (1997).

Acknowledgements. We thank J. Sedat and D. Agard for use of their CCD-based optical sectioning microscope and image processing facilities; R. P. Jansen and K. Nasmyth for strains; E. O'Shea for plasmids; and D. Drubin for latrunculin A. This work was supported by grants from the NIH (R.D.V. and I.H.) and a grant from the Cancer Research Fund of the Damon Runyon–Walter Winchell Foundation Fellowship (J.R.S.).

Correspondence and requests for materials should be addressed to R.D.V. (e-mail: vale@phy.ucsf.edu).

Reversal in the direction of movement of a molecular motor

Ulrike Henningsen & Manfred Schliwa

Adolf-Butenandt-Institut, Zellbiologie, University of Munich, Schillerstrasse 42, 80336 Munich, Germany

Kinesin and non-claret disjunctional (ncd) are molecular motors of the kinesin superfamily that move in opposite directions along microtubules. The molecular basis underlying the direction of movement is unclear, although it is thought to be an intrinsic property of the motor domain, a conserved region about 330 amino acids in length[1–3]. The motor domain is found at the amino terminus in conventional kinesins, but at the carboxy terminus in ncd[4,5]. Here we report on a chimaera composed of the motor domain of the minus-end-directed kinesin of *Neurospora crassa*[6]. The bacterially expressed fusion protein was tested in motility assays using polarity-marked microtubules[7]. Surprisingly, the chimaera moved towards the plus end, demonstrating that the polarity of force generation of the ncd motor domain has been reversed. This finding indicates that the domain organization, particularly the position of the motor domain, is of fundamental importance for the polarity of force production. It also demonstrates that the direction of microtubule movement is not controlled solely by the motor domain[8].

The molecular motor non-claret disjunctional (ncd) is a member of the kinesin superfamily that moves towards the minus end of microtubules. It consists of an N-terminal tail region of ~200 amino acids, a central stalk with heptad repeats, as in the stalk of conventional kinesin, and a C terminus that contains a region (residues 348–670) that is 41% identical to the motor domain of other kinesins[5,9]. We constructed a chimaera in the vector pt7-7 (ref. 10) consisting of the motor domain of ncd derived from glutathione *S*-transferase (GST)–MC5 (ref. 11) fused to the N terminus of the stalk/tail domain of *Neurospora* kinesin (Nkin). In this chimaera, the first amino acid is Met 333 of the ncd sequence (numbering according to ref. 9), and the splice site is within the codon for Leu 661 in ncd (Leu 321 in Nkin). This leucine is located in a conserved region of the helix α6, which is identical in length and position in the crystal structures of kinesin and ncd[12]. Therefore, neither the length nor the characteristics of this helix are expected to change in the chimaera. The juncture is located seven amino acids N-terminal to the end of the conserved motor domain of most kinesins[1,2,12]. The resulting product, which showed the splice site in the expected position (Fig. 1), was sequenced and shown to be free of error. A set of digests of the chimaera with appropriate restriction enzymes, as well as polymerase chain reactions (PCR) using internal primers, all yielded the expected products (not shown), supporting the conclusion that the plasmid was constructed as we thought.

The ncd–Nkin chimaera was expressed in *Escherichia coli*. Induction with IPTG yielded large amounts of a soluble polypeptide with a relative molecular mass of about 105,000 (M_r 105K), which is of the expected size for the ncd–Nkin chimaera. This polypeptide could be purified by a microtubule affinity step in the presence of apyrase and the non-hydrolysable ATP analogue AMP-PNP (Fig. 2). The material released from microtubules by ATP (S5) consisted almost exclusively of the 105K polypeptide, with contamination from tubulin. Thus this polypeptide exhibited the ATP-dependent microtubule binding and release behaviour typically of microtubule motors. Its behaviour on a Superose 6 gel-filtration column was very similar to that of bacterially expressed Nkin, and suggests that the

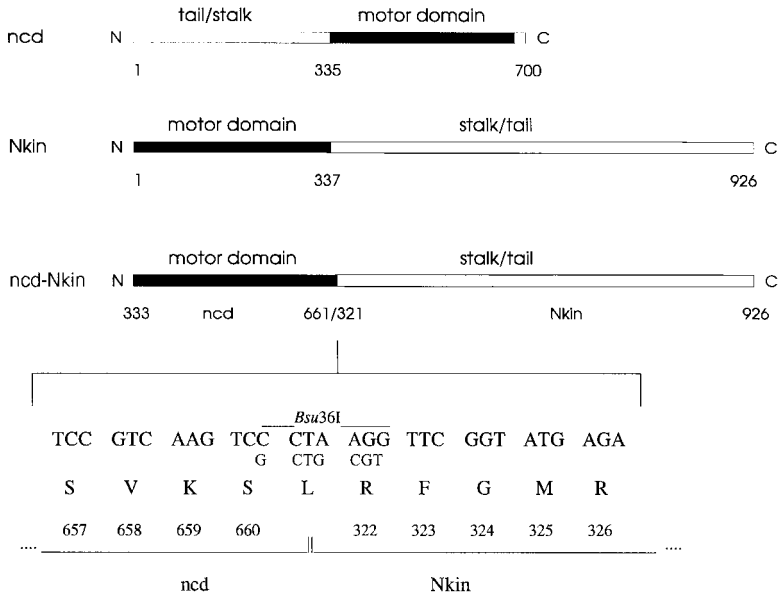

Figure 1 Overview of the domain organization of the non-claret disjunctional motor (ncd), *Neurospora* kinesin (Nkin), and the chimaera (ncd–Nkin). The nucleotide sequence of the head/stalk transition of ncd–Nkin (as determined by sequencing of the construct) is shown at the bottom. The *Bsu*36I site generated by site-directed mutagenesis is indicated, along with the original nucleotide sequences, shown in smaller print. The codon for Leu661/321 is CTG in both ncd and Nkin.